

Gab1 regulates SDF-1-induced progression via inhibition of apoptosis pathway induced by PI3K/AKT/Bcl-2/BAX pathway in human chondrosarcoma

Yongqian Fan¹ · Fengjian Yang¹ · Xuhai Cao¹ · Cong Chen¹ · Xuelin Zhang¹ · Xu Zhang¹ · Weilong Lin¹ · Xiaofeng Wang² · Chengwei Liang¹

Received: 18 June 2015 / Accepted: 20 July 2015 / Published online: 16 August 2015
© International Society of Oncology and BioMarkers (ISOBM) 2015

Abstract In recent decades, the stromal cell-derived factor-1 (SDF-1) and Gab1 have been investigated to be involved in oncogenesis. However, it is scarcely reported that SDF-1-Gab1 pathway mediates proliferation and apoptosis in human chondrosarcoma (CS). In this study, we assessed the expression of Gab1 in 90 CS solid tumors by immunohistochemistry, immunoblotting, and qRT-PCR, and then, some in vitro assays were also applied to CS cells treated with SDF-1. We observed that the overexpression of Gab1 was positively correlated with lung metastasis and recurrence, and acts as an independent prognostic factor for CS patients. Gab1 expression was up-regulated in response to SDF-1 stimulation in CS cell line JJ012, SW1353, L3252. Overexpression of Gab1 increased Bcl-2/BAX ratio to promote cell growth via PI3K/AKT. On the other hand, silencing of Gab1 accelerated apoptosis and repressed the growth of CS cells, which further caused the inhibition of G1/S phase transition and decreased invasion capacity in CS cell lines. In vivo assay identified that the knockdown of Gab1 interfered with the tumor mass formation. In conclusion, our data identified overexpression of Gab1 in CS tissues, and Gab1 can be recommended as a novel

biomarker for diagnosis and prognosis in patients with CS. Additionally, PI3K/AKT/Bcl-2/BAX axis was involved in Gab1-induced CS progression, indicating Gab1 might act as a new target for the treatment of CS patients.

Keywords Gab1 · SDF-1 · Human chondrosarcoma · Apoptosis

Introduction

Chondrosarcoma acts as one of the most common malignant cartilaginous tumors due to malignant invasion property [1, 2]. The classical treatment option includes surgical resection, chemotherapy, and radiotherapy [3, 4]. In recent years, some novel approaches to CS patients remain unsatisfactory because the postoperative patients often have the recurrence of CS, even death. Thus, the most important way to treat CS patients should be the early definitive diagnosis [5]. In recent decades, EMT has been widely reported as an initiation process in CS development, while the specific mechanisms involved in EMT of CS is still unclear.

Gab1, Grb2-associated binding protein 1, is implicated in the progression of different tumors involving digestive duct tumors [6–9]. Gab1 acts as an adapter protein that is involved in the signal transduction of different factors [10]. As reported, Gab1 can be expressed in many human organs and can interact with PIP3, PI3K, Grb2, and SHP2 to exert various biological effects and behaviors [11, 12]. At the same time, SDF-1 signaling also plays an important role in tumorigenesis, which promotes some important pathological events [13, 14]. Several signaling pathways stimulated by SDF-1 can promote the proliferation, migration, and even apoptosis of CS.

In this study, we analyzed the role of Gab1 in CS by analyzing their expression in CS tumor tissues and their

Yongqian Fan, Fengjian Yang, and Xuhai Cao contributed equally to this work as co-first authors.

- ✉ Xiaofeng Wang
shwangxiaofeng@163.com
- ✉ Chengwei Liang
liangcweish126@163.com

¹ Department of Orthopedics, Huadong Hospital Affiliated to Fudan University, No. 221 West Yan An Road, Shanghai 200040, China
² Department of Orthopedics, Zhongshan Hospital Affiliated to Fudan University, No. 136 Xue Yuan Road, Shanghai 200032, China

association with clinical and pathological characteristics. We further investigated the role of Gab1 in the malignant behavior of the CS cell lines.

Materials and methods

Patients and tissue samples

In our study, 90 cases of CS tissues were enrolled from the Department of Pathology at Huadong Hospital Affiliated to Fudan University between January 2006 and June 2010. A total of 65 men and 25 women were included with an average age of 42.1 years (age range 26–51 years). If a patient was identified with previous treatment of radiochemotherapy, surgery must not be considered. As for non-neoplastic tissues, we obtained these tissues at 2 to 5 cm distance from the edge of cancer tissues. All tissues were divided into sections, fixed in 4 % buffered formalin, and then embedded in paraffin. Before our scientific research, we obtained patient's approval through the Ethics Committee of Huadong Hospital Affiliated to Fudan University. To point out, follow-up information was also acquired by way of phone or family visit. The duration of follow-up ranged from 2 to 100 months.

Immunohistochemistry

Immunohistochemical staining was performed using antibodies as mentioned above (1:500 titers). Paraffin-embedded sections (5 μ m) were dewaxed in xylene and rehydrated using graded ethanol. Sections were incubated in 3 % hydrogen peroxide for 10 min to inactivate endogenous peroxidases. Then, the sections were heated (at 100 °C) for 15 min in 0.01 mol/L citrate buffer, then cooled for 30 min at room temperature to expose antigenic epitopes. The sections were blocked with 2 % normal goat serum in PBS for 30 min and then incubated overnight at 4 °C with primary antibody. Using the EnVision System-labeled HRP antimouse (Dako, Denmark), the primary antibody was visualized with diaminobenzidine-H₂O₂ and counterstained with Mayer's hematoxylin. PBS was used instead of the primary antibodies for the negative controls.

Cell culture and reagents

Human JJ012, SW1353, and L3252 cells were purchased from the Chinese Academy of Sciences. All cells were cultured in DMEM (Gibco) containing 10 % fetal bovine serum at 37 °C, and 5 % CO₂, and passaged every 3 days. Cells in the logarithmic growth phase were used for experiments. RNA simple Total RNA Kit and TIAN Script RT Kit were purchased from Tiangen Biotech Beijing Co., Ltd. Each experiment was repeated in triplicate.

Cell transfection

The wild-type and mutant Gab1 cDNA was constructed with the help of Beijing DingSheng Corp. Ltd. The wild-type or mutant Gab1-expressing plasmid was transfected into all indicated CS cells using FuGENE6 transfection reagent (Promega, Madison, USA) as Gab1-expressing CS cells. Stable transfection clones were obtained after 2-week selection.

Gab1 siRNA treatment

Gab1 and control siRNA interference sequences were available from GenBank. siRNA was a generous gift from Dr. Wang (Chinese Science Academy, Beijing, China). siRNAs were transfected into cells using lipofectamine 2000 (Invitrogen) according to the manufacturer's instructions.

Western blotting

After treatment, cells were washed with precold PBS and lysed with RIPA buffer containing the protease inhibitor and phosphatase inhibitor cocktails. Protein concentrations were measured by Pierce BCA protein assay kit. An equal amount of protein sample (20 μ g) was electrophoresed on 7 or 12 % sodium dodecyl sulfate polyacrylamide gel electrophoresis mini-gel after thermal denaturation for 5 min at 95 °C. Following that, proteins were transferred onto methanol-activated PVDF membrane at 100 V for 2 h at 4 °C. Subsequently, membranes were blocked with 5 % skim milk and probed with indicated primary antibody overnight at 4 °C and then blotted with respective secondary antibody. Visualization was performed using Bio-Rad system. The blots were analyzed using ImageLab 3.0 (Bio-Rad) and protein level was normalized to the matching densitometric value of β -actin.

Reverse transcription polymerase chain reaction (RT-PCR)

Total RNA was extracted from cells, and gene expression was investigated using RT-PCR kit according to the manufacturer's instructions. At the same time, PCR was also carried out for 30 cycles of denaturation (30 s at 94 °C), annealing (40 s at 55 °C), and extension (30 s at 72 °C). The PCR products were then separated on 1 % agarose gel containing 0.5 g/ml ethidium bromide. The gel was put on an UV transilluminator and photographed. The signal was measured by a densitometer and standardized against the β -actin signal using a digital imaging and analysis system.

Cell viability and cell proliferation assay

3-(4, 5-Dimethylthiazol-2-yl)-2, 5-diphenyltetrazolium bromide (MTT) assay was conducted to examine cell viability. CS cells were plated at the concentration of 5000 cells per well in a 96-well plate and cultured for 24 h in a humidified 5 % CO₂, 95 % air atmosphere at 37 °C. Twenty microliters of MTT (5 mg/ml) solution from Sigma-Aldrich Co. (St. Louis, USA) was added to each well. After incubation for 4 h at 37 °C, we removed the culture medium and added 200 µl of dimethyl sulfoxide to dissolve the formazan. After incubation for 30 min at room temperature, the cell culture plates were scanned with a microplate reader at 570 nm to assess the absorbance. CS cells were seeded into 96-well plates at 5000 cells per well for 24 h, and the BrdU ELISA assay (BrdU ELISA from Roche, Indianapolis, USA) was performed to measure cell proliferation. All experiments were repeated at least three times.

Transwell assay

Twenty-four hours after transfection, cells were used for migration and invasion assays. Transwell migration assay was carried out in 24-well plates using costar transwell assay kit (3422; Corning, USA). The invasion assay was carried out using invasion chambers (354480; BD, USA) pre-coated with Matrigel. Cells (2.0×10⁵ per well) were seeded in the upper chamber, and medium containing SDF-1 was added to the lower chamber. After 48 h of incubation at 37 °C in 5 % CO₂, noninvasive cells were removed from the upper surface of the transwell membrane with a cotton swab, and the migrated or invaded cells on the lower membrane surface were fixed, stained, photographed, and counted under high-power magnification (×200).

In vivo studies

Animal studies were performed according to institutional guidelines. JJ012 cell lines were transfected in vitro. At 24 h after the transfection, viable cells were injected into the left flanks of 5-week-old female nude mice, five mice per transfected or control cell line. Tumor diameters were measured on week 1, 2, 2.5, 3, 3.5, and 4. After 28 days, the mice were killed, necropsies were performed, and tumors were weighed. Tumor volumes were calculated by using the equation $V(\text{mm}^3) = A \times B^2 / 2$, where A indicates the largest diameter and B indicates the perpendicular diameter.

Statistical analysis

The SPSS19 software package was used for statistical analysis. All data were presented as the mean±SEM. Student's t test (for data with a normal distribution) or Mann–Whitney U test

(for data with a non-normal distribution) was used for comparing means between two groups. Differences were considered statistically significant when $p < 0.05$.

Results

Gab1 is highly expressed in CS tissues

As shown in Table 1, Gab1 was highly expressed in CS tissues in comparison with non-tumor tissues as determined by immunohistochemistry. According to measurement, Gab1 expression levels in CS cancer tissues were 0.2098±0.0051, which was significantly higher than that in normal tissues (0.1811±0.0047) ($p < 0.001$). Besides, intracellular localization of Gab1 was defined into the cell cytoplasm and membrane in cancer cells. IHC results indicated Gab1 expression was induced and up-regulated in CS development.

Based on these data, we summarized the correlations with clinicopathological parameters. We found that the overexpression of Gab1 was decreased in low grade CS, while it increased on high grade CS. Differences were significant ($p < 0.01$; Table 1). In addition, the positive rate of Gab1 in patients with recurrence was significantly higher than those in patients without recurrence ($p < 0.01$; Table 1). As for age and gender, we did not find any associations with Gab1 expression. Besides, we identified the correlations of high Gab1 expression with CS grade and recurrence using Western blotting, RT-PCR (Fig. 1a, b), and qRT-PCR (Fig. 1c).

Table 1 Association of Gab1 expression with clinicopathological parameters

Parameters	Number	OD value of Gab1	p value
Age			
<42	45	0.208±0.004	0.545
≥42	45	0.209±0.003	
Gender			
Female	29	0.210±0.005	0.124
Male	61	0.209±0.004	
Recurrence			
Yes	55	0.215±0.003	0.001
No	35	0.205±0.004	
Grade			
High	53	0.218±0.004	0.001
Low	37	0.206±0.003	
Lung metastasis			
Yes	56	0.216±0.005	0.000
No	34	0.206±0.004	

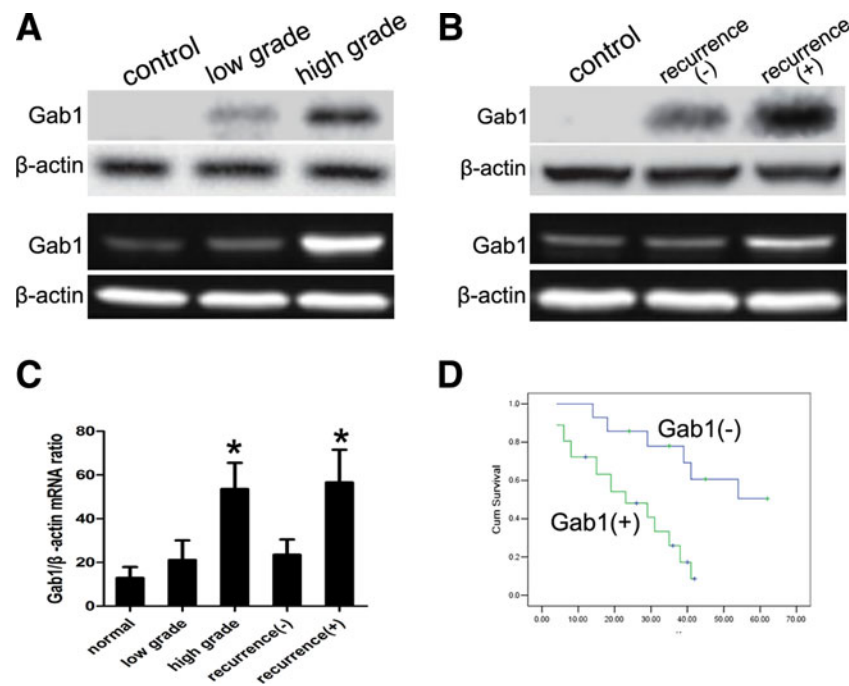


Fig. 1 Expression and significance of Gab1 in human chondrosarcoma samples. RT-PCR and Western blotting (**a**, **b**) analysis was performed in 90 cases of CS tissues, and identified the expression of Gab1 in human CS tissues that was positively correlated with grade and recurrence. β -Actin acts as an internal control. **c** qRT-PCR identified the expression

of Gab1 in human CS tissues. Each bar represents the mean \pm SEM; $*p < 0.001$, compared with control, one-way ANOVA. **d** The overall survival curves are shown for a total of 80 CS patients. High Gab1 expression was obviously associated with a 5-year prognosis using log-rank test ($p < 0.000$)

Gab1 expression in CS tissues is an independent prognostic factor

The follow-up information was obtained from 80 of 90 CS cases with the median time of 21 months. The 80 CS patients were divided into two groups: high Gab1 and low/non-Gab1 expression using the median ratio of tumor/benign Gab1 expression as the cut-off value. We studied relationships of Gab1 expression with overall survival of CS patients using Kaplan–Meier analysis, log-rank test, and Cox proportional hazard models. As shown in Fig. 1d, patients whose tumors expressing Gab1 had shorter median overall survival period than those whose tumors expressed Gab1 (18.0 vs. 29.0 months; log-rank test, $p < 0.000$, respectively). As shown in Table 2,

after univariate analysis, it was found that grade, recurrence, lung metastasis, and higher Gab1 expression in CS tissues were the poor prognostic factors. Furthermore, multivariate analysis revealed that recurrence, lung metastasis, and higher Gab1 expression in CS tissues were the independent prognostic factors for CS patients. Thus, Gab1 expression was recommended as an independent valuable predicting factor in clinical practice.

Enhanced expression of Gab1 represses CS cell apoptosis and accelerated CS cell growth

To figure out the role of Gab1 in CS progression, we examined Gab1 in CS cells, involving JJ012, SW1353,

Table 2 Univariate and multivariate analyses of prognostic indicators in CS patients

Indicators	Univariate		Multivariate	
	HR (95 % CI)	<i>p</i>	HR (95 % CI)	<i>p</i>
Age (<42/≥42)	0.62 (0.14–2.69)	0.523	NA	NA
Gender (male/female)	1.71 (0.22–13.51)	0.611	NA	NA
Lung metastasis (yes/no)	2.23 (1.20–4.14)	0.011	1.98 (1.09–3.60)	0.025
Grade (high/low)	2.09 (1.20–3.63)	0.009	1.59 (0.84–4.16)	0.125
Recurrence (yes/no)	2.23 (1.49–3.38)	<0.000	2.05 (1.22–3.79)	0.008
Gab1 (+–+++/-)	2.31 (1.51–3.45)	<0.000	2.11 (1.19–3.82)	0.011

and L3252. Both qRT-PCR and immunoblotting assay showed that there was moderate expression level of Gab1 expression in JJ012, SW1353, and L3252 (Fig. 2a, b). Therefore, we transduced all CS cells with empty vector, wild-type Gab1, or mutant Gab1-expressing plasmid stably to establish CS vector and CS Gab1-WT or MT cells. Subsequently, qRT-PCR and immunoblotting assay identified Gab1 expression was significantly up-regulated in CS Gab1 cells compared to CS vector and Gab1-MT cells (Fig. 2a, b). DAPI staining assay also showed that the rate of DAPI staining cells was approximately 8 % in JJ012 Gab1 cells, which was significantly lower than 32 % in JJ012 vector cells (Fig. 2c). At the same time, overexpression of Gab1 reduced the caspase 3/7 activity by approximately three fourths in JJ012 cells. Furthermore, we carried out BrdU incorporation and MTT assay to elucidate the function of Gab1 in CS cell growth. Consistent with the results of cell apoptosis, there was about

a half increase in BrdU incorporation in CS cells after Gab1 overexpression (Fig. 2d). MTT assay also showed that enhanced expression of Gab1 increased CS cell viability as shown in Fig. 3a; however, Gab1-MT affected the CS cell viability.

Knockdown of Gab1 suppresses cell growth and induces cell apoptosis

To confirm the effect of Gab1 on cell proliferation and apoptosis, we silenced Gab1 expression in JJ012, SW1353, and L3252 cells by targeting siRNA sequences (Fig. 3b). We examined cell proliferation and growth capacities as well. All cell viability was repressed significantly at 48 and 72 h clearly after knock-down of Gab1 in CS cells, as shown in Fig. 3b. Next, we determined whether Gab1 can regulate apoptosis of CS cells. The percentage of apoptotic cells was lower in

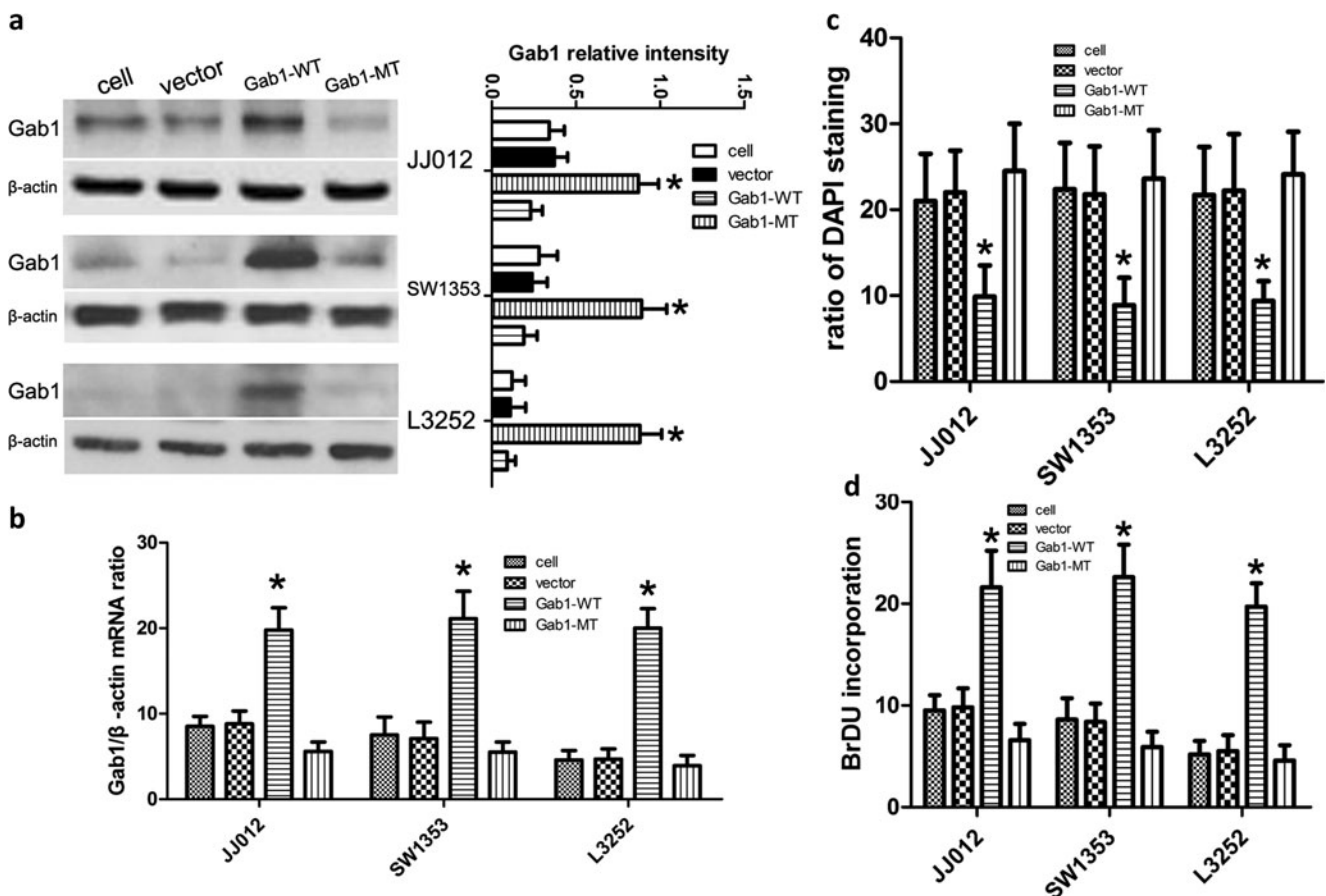


Fig. 2 Enforced expression of Gab1 represses cell apoptosis and accelerated CS cell growth. **a, b** As assessed by both Western immunoblotting and qRT-PCR assays, it was found that there was low and moderate Gab1 expression in JJ012, SW1353, and L3252 cells. There was significantly more Gab1 expression in CS cell stably transfected with Gab1-expressing plasmid than ones transfected with

control or mutant plasmid, as examined by both Western immunoblotting and qRT-PCR assays. **c** DAPI staining assay showed the percentage of apoptotic cell in CS cells treated above. BrdU incorporation assay showed that enforced expression of Gab1 promoted cell proliferation in JJ012, SW1353, and L3252 cells. Each bar represents the mean \pm SEM; * p < 0.001, compared with control, one-way ANOVA

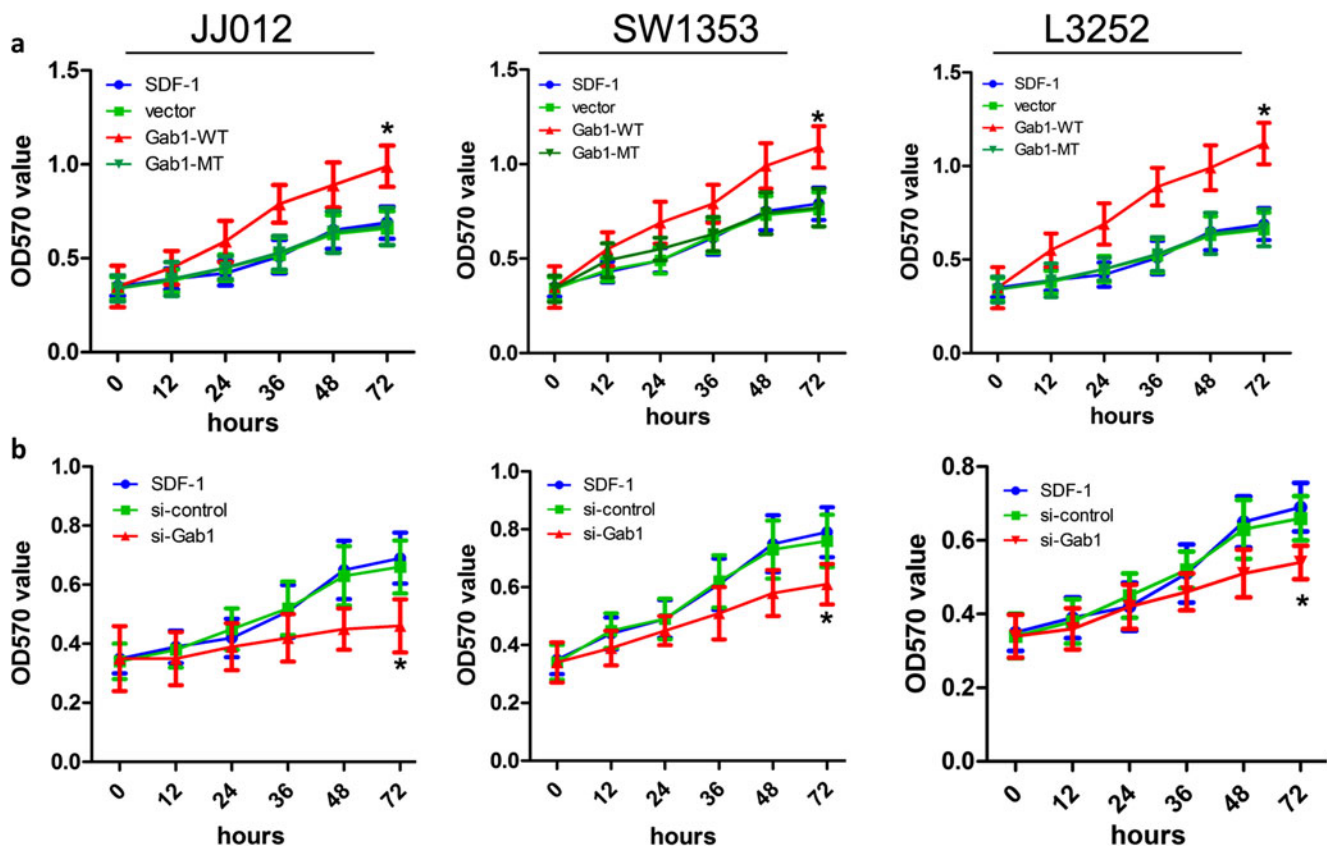


Fig. 3 The effect of knockdown of Gab1 on cell growth in CS cells. **a** As assessed by the MTT assay, cell growth and viability were increased at 24, 48, and 72 h by overexpression of Gab1 in CS cells. **b** Compared with

cells transfected with the control siRNA, the growth rate of CS cells was significantly decreased after Gab1 siRNA interference, $*p < 0.01$, compared with control, one-way ANOVA

the si-control-treated cells than that in the si-Gab1-treated cells (Fig. 4).

Gab1 increases the ratio of Bcl-2/BAX via activating PI3K/AKT signaling

To explore the underlying mechanism underlying Gab1-induced cell apoptosis in CS cells, we explored the involvement of PI3K/AKT pathway in Gab1-induced growth and apoptosis. Immunoblotting revealed that overexpression of Gab1 in JJ012 cells induced the higher expression of PI3K p101 protein and AKT phosphorylation (Fig. 5a). Furthermore, we observed Bcl-2 expression can be up-regulated and BAX expression can be inhibited in CS Gab1 cells instead of CS vector cells (Fig. 5a). Accordingly, silencing of Gab1 repressed PI3K p101 expression and phosphorylation of AKT and decreased the ratio of Bcl-2/BAX in CS cells (Fig. 5a). These data supported strongly that Gab1 enforced Bcl-2/BAX ratio via increasing phosphorylation of AKT and consequently exerted its anti-apoptotic effects in CS progression.

Knockdown of Gab1 results in G1 phase arrest and inhibits cell invasion

To elucidate the mechanism underlying SDF-1/Gab1/PI3K/Akt-regulated cell growth in CS cells, we carried out flow cytometry in JJ012 cells. Compared with the control siRNA, following transfection of si-Gab1, there was a significant increase in the percentage of CS cells in the G1 phase ($p < 0.01$), a significant decrease in proportion of CS cells in the S phase ($p < 0.01$), and no significant change in the G2 phase (Fig. 5b). These findings indicated that knockdown of Gab1 in CS cells led to G1/S phase arrest. Additionally, as shown in Fig. 5c, the invasive capacity of cells was significantly decreased after Gab1 knockdown ($p < 0.01$). These findings indicate that the SDF-1/Gab1/PI3K/Akt pathway can modulate the invasive capacity of CS cells.

The knockdown of Gab1 inhibits tumor formation in vivo

To properly figure out the in vivo effects of Gab1, we used JJ012 cells with transfectant Gab1-WT or Gab1-MT, which were embedded into the subcutaneous tissues of nude mice.

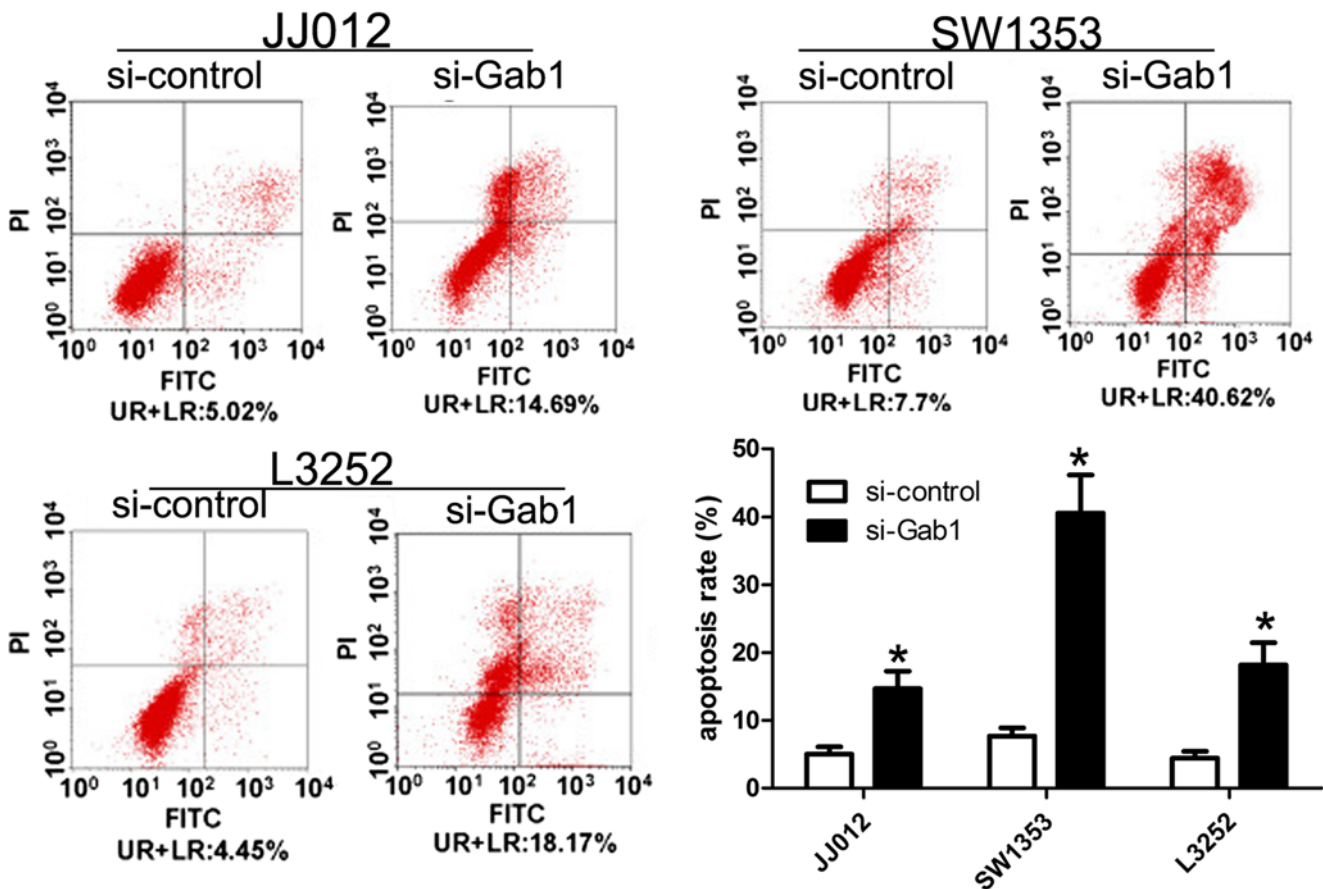


Fig. 4 The effect of knockdown of Gab1 cell cycle in CS cells. Cell cycle was detected using PI staining and flow cytometry. The apoptosis proportion of CS cells in si-Gab1-treated cells was significantly

increased. Results shown are the mean±SEM of repeated independent experiments. * $p < 0.01$, compared with control, one-way ANOVA

As shown in Fig. 6, after 28 days, the mutant Gab1 inhibits the size and weight of tumor mass derived from JJ012 cells (Fig. 6). At day 28, the average weights of the parental and vector-treated nude mice were 85 ± 5 and 87 ± 4 mg, respectively. However, in nude mice treated with Gab1-WT or Gab1-MT cells, the average weight was defined as 110 ± 11 and 55 ± 6 mg, respectively, and the difference is significant ($p < 0.001$). So, our data demonstrate that the knockdown of Gab1 inhibits CS tumor formation in vivo.

Discussion

It has been reported that Gab1 is shown to interact with tyrosine phosphatase SHP2 and to promote cardiac hypertrophy. Also, Gab1 is essential for cardiac function in the postnatal heart in vivo. In addition, Gab1 has been shown to exert an anti-apoptotic role in mouse embryonic fibroblasts and is activated through tyrosine phosphorylation following oxidative treatment (H_2O_2). In the present study, we demonstrated that SDF-1-

Gab1 pathway is involved in CS progression via activation of the PI3K/Akt signaling pathway.

Firstly, we used immunohistochemistry and observed a high expression of Gab1 in CS tissues from 90 patients and identified that Gab1 was associated with lung metastasis and grade. The aforementioned results indicated that Gab1 is implicated in malignant transformation of CS cancers. Consistent with our study, Gab1 is critical for SDF-1-mediated tumor angiogenesis and lymphangiogenesis, and its expression is associated with other tumor invasion and metastasis [15, 16].

Next, we determined the role of Gab1 on CS progression and transfected all CS cells with empty vector, wild-type Gab1, or mutant Gab1-expressing plasmid stably to establish CS vector and CS Gab1-WT or MT cells. We found that the expression of Gab1 was significantly up-regulated in CS Gab1 cells compared to CS vector and Gab1-MT cells. DAPI staining assay showed the percentage of DAPI staining cells in CS Gab1 cells was remarkably lower than that in vector cells. It was also found that ectopic expression of Gab1 reduced the caspase 3/7 activity, indicating Gab1 promotes cell viability.

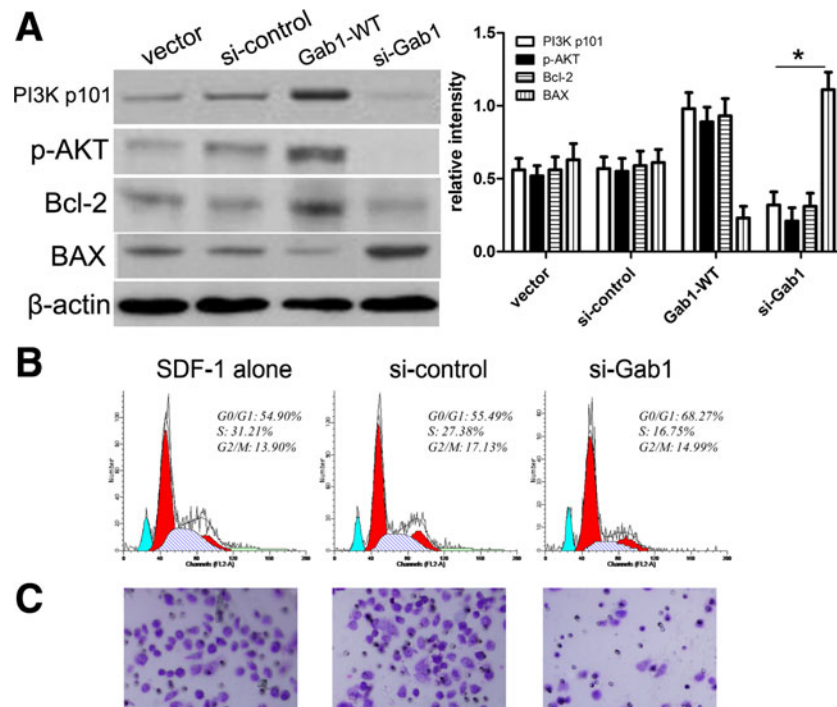


Fig. 5 Gab1 affects the ratio of Bcl-2/BAX, cell cycle, and invasion. **a** As assessed by Western immunoblotting, enhanced expression of Gab1 increased PI3K p101 expression, AKT phosphorylation, and Bcl-2 expression, and decreased BAX expression in CS cells. Knockdown of Gab1 suppressed PI3K p101 expression and phosphorylation of AKT and

decreased the ratio of Bcl-2/BAX in JJ012 cells. **b** Cell cycle was detected using PI staining and flow cytometry, and the proportion of RBE cells in G1 phase was significantly increased. **c** Cell invasion was detected using a transwell invasion assay

Furthermore, we conducted BrdU incorporation and MTT assay to find that there was around a half increase in BrdU incorporation in CS cells after Gab1 overexpression, and enhanced expression of Gab1 increased viability of all CS cells at all four time points clearly.

In the present study, our results also demonstrated that the SDF-1-Gab1 signaling pathway contributes to the malignant behavior of CS. We tested their tumor-suppression function in vivo. The mutant Gab1 inhibits the growth of JJ012 tumor engraftments, while the overexpression of Gab1 promotes

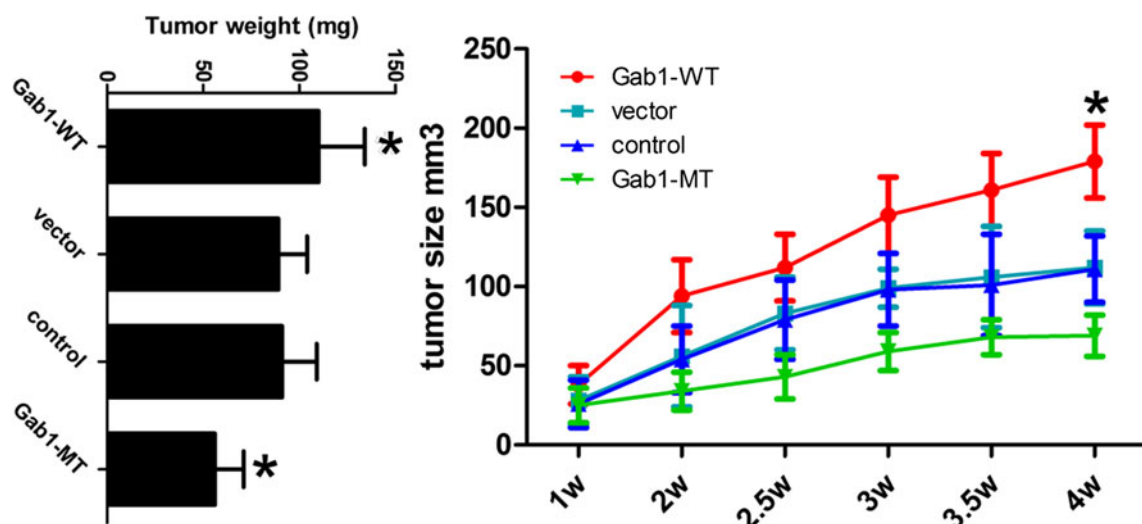


Fig. 6 In vivo effects of Gab1 on JJ012 cells knockdown of Gab1 inhibits the growth of JJ012 tumor engraftments in nude mice. Growth curve of engrafted tumors was recorded in weeks in nude mice injected

with JJ012 cells pre-treated with transfection. Comparison of tumor engraftment sizes was conducted at 28 days after injection in nude mice. Tumor weights±SEM in nude mice

tumor formation. The results of these experiments demonstrate the tumor-suppressor function of knockdown of Gab1 in CS cells.

In summary, this study identified that Gab1 was aberrantly overexpressed in CS and acts as a poor prognostic marker. Additionally, PI3K/AKT/Bcl-2/BAX axis was involved in Gab1-induced CS progression, indicating that Gab1 might act as a new target for the treatment of CS patients.

Acknowledgments We thank all the patients who were willing to be recruited in this investigation. At the same time, we thank other members in our laboratory for valuable suggestions and writing.

Conflicts of interest None

References

1. Leddy LR, Holmes RE. Chondrosarcoma of bone. *Cancer Treat Res.* 2014;162:117–30.
2. Azzi G, Velez M, Mathias-Machado MC. Isocitrate dehydrogenase mutations in chondrosarcoma: the crossroads between cellular metabolism and oncogenesis. *Curr Opin Oncol.* 2014;26:403–7.
3. DeLaney TF, Liebsch NJ, Pedlow FX, et al. Long-term results of phase II study of high dose photon/proton radiotherapy in the management of spine chordomas, chondrosarcomas, and other sarcomas. *J Surg Oncol.* 2014;110:115–22.
4. Frezza AM, Cesari M, Baumhoer D, et al. Mesenchymal chondrosarcoma: prognostic factors and outcome in 113 patients. A European Musculoskeletal Oncology Society study. *Eur J Cancer.* 2015;51:374–81.
5. Gherman V, Tomuleasa C, Bungardean C, et al. Management of renal extraskelatal mesenchymal chondrosarcoma. *BMC Surg.* 2014;14:107.
6. Yamasaki S, Nishida K, Yoshida Y, et al. Gab1 is required for EGF receptor signaling and the transformation by activated ErbB2. *Oncogene.* 2003;22:1546–56.
7. Gillgrass A, Cardiff RD, Sharan N, et al. Epidermal growth factor receptor-dependent activation of Gab1 is involved in ErbB2-mediated mammary tumor progression. *Oncogene.* 2003;22:9151–5.
8. Seiden-Long I, Navab R, Shih W, et al. Gab1 but not Grb2 mediates tumor progression in Met overexpressing colorectal cancer cells. *Carcinogenesis.* 2008;29:647–55.
9. Sang H, Li T, Li H, et al. Down-regulation of Gab1 inhibits cell proliferation and migration in hilar cholangiocarcinoma. *PLoS One.* 2013;8:e81347.
10. Gu H, Neel BG. The BGab⁺ in signal transduction. *Trends Cell Biol.* 2003;13:122–30.
11. Nishida K, Hirano T. The role of Gab family scaffolding adapter proteins in the signal transduction of cytokine and growth factor receptors. *Cancer Sci.* 2003;94:1029–33.
12. Wöhrle FU, Daly RJ, Brummer T. Function, regulation and pathological roles of the Gab/DOS docking proteins. *Cell Commun Signal.* 2009;7:22.
13. Shi J, Wei Y, Xia J, et al. CXCL12-CXCR4 contributes to the implication of bone marrow in cancer metastasis. *Future Oncol.* 2014;10(5):749–59.
14. Nagasawa T. CXC chemokine ligand 12 (CXCL12) and its receptor CXCR4. *J Mol Med (Berl).* 2014;92(5):433–9.
15. Yamashita J, Itoh H, Hirashima M, Ogawa M, et al. Flk1-positive cells derived from embryonic stem cells serve as vascular progenitors. *Nature.* 2000;408:92–6.
16. Hirakawa S, Kodama S, Kunstfeld R, et al. VEGF-A induces tumor and sentinel lymph node lymphangiogenesis and promotes lymphatic metastasis. *J Exp Med.* 2005;201:1089–99.